Early Effects of Salinity on Water Transport in Arabidopsis Roots. Molecular and Cellular Features of Aquaporin Expression[1]

Yann Boursiac[2], Sheng Chen[2,3], Doan-Trung Luu, Mathias Sorieul, Niels van den Dries, and Christophe Maurel*

Biochimie et Physiologie Moléculaire des Plantes, Agro-Montpellier/Centre National de la Recherche Scientifique/Institut National de la Recheche Agonomique/Université Montpellier 2, Unité Mixte de Recherche 5004, F–34060 Montpellier cedex 1, France

Aquaporins facilitate the uptake of soil water and mediate the regulation of root hydraulic conductivity (L_{p_r}) in response to a large variety of environmental stresses. Here, we use Arabidopsis (*Arabidopsis thaliana*) plants to dissect the effects of salt on both L_{p_r} and aquaporin expression and investigate possible molecular and cellular mechanisms of aquaporin regulation in plant roots under stress. Treatment of plants by 100 mM NaCl was perceived as an osmotic stimulus and induced a rapid (half-time, 45 min) and significant (70%) decrease in L_{p_r}, which was maintained for at least 24 h. Macroarray experiments with gene-specific tags were performed to investigate the expression of all 35 genes of the Arabidopsis aquaporin family. Transcripts from 20 individual aquaporin genes, most of which encoded members of the plasma membrane intrinsic protein (PIP) and tonoplast intrinsic protein (TIP) subfamilies, were detected in nontreated roots. All PIP and TIP aquaporin transcripts with a strong expression signal showed a 60% to 75% decrease in their abundance between 2 and 4 h following exposure to salt. The use of antipeptide antibodies that cross-reacted with isoforms of specific aquaporin subclasses revealed that the abundance of PIP1s decreased by 40% as early as 30 min after salt exposure, whereas PIP2 and TIP1 homologs showed a 20% to 40% decrease in abundance after 6 h of treatment. Expression in transgenic plants of aquaporins fused to the green fluorescent protein revealed that the subcellular localization of TIP2;1 and PIP1 and PIP2 homologs was unchanged after 45 min of exposure to salt, whereas a TIP1;1-green fluorescent protein fusion was relocalized into intracellular spherical structures tentatively identified as intravacuolar invaginations. The appearance of intracellular structures containing PIP1 and PIP2 homologs was occasionally observed after 2 h of salt treatment. In conclusion, this work shows that exposure of roots to salt induces changes in aquaporin expression at multiple levels. These changes include a coordinated transcriptional down-regulation and subcellular relocalization of both PIPs and TIPs. These mechanisms may act in concert to regulate root water transport, mostly in the long term (≥6 h).

Soil salinity exerts noxious effects on plants and causes a significant drop in yield for crop production in 7% of arable land worldwide, including the majority of irrigated lands (Hasegawa et al., 2000; Halperin et al., 2003; Zhu, 2003). In particular, exposure to salinity challenges the plant water status and triggers specific strategies for cell osmotic adjustment and control of water uptake and loss (Hasegawa et al., 2000; Fricke and Peters, 2002). One of the primary responses of plants to salt is inhibition of their root water uptake capacity (i.e. root hydraulic conductivity [L_{p_r}]). Although notable exceptions have been reported in barley (*Hordeum vulgare*; Munns and Passioura, 1984) and tobacco (*Nicotiana tabacum*; Tyerman et al., 1989), this response can be observed in a large variety of glycophytic and halophytic plant species, including Arabidopsis (*Arabidopsis thaliana*; Azaizeh and Steudle, 1991; Peyrano et al., 1997; Carvajal et al., 1999; Martinez-Ballesta et al., 2000, 2003).

The notion that aquaporin water channels serve as a major path for uptake of water by roots was raised from early experiments showing that root water transport can be inhibited by the general aquaporin blockers, mercury ions (for review, see Javot and Maurel, 2002). It was also shown in several plant species that the residual L_{p_r} observed after salt treatment was insensitive to mercury inhibition, suggesting that aquaporin down-regulation is the primary cause of salt-induced reduction in L_{p_r} (Carvajal et al., 1999; Martinez-Ballesta et al., 2000, 2003). Recent physiological and genetic studies have confirmed conclusions based on mercury inhibition and provide compelling evidence for a role of aquaporins in the regulation of water transport under stress (Martre et al., 2002;

[1] This work was supported in part by Génoplante (grant no. AF–2001065) and by the Centre National de la Recherche Scientifique (Action Thématique Incitative sur Programme et Equipe "Function and regulation of plant aquaporins"). S.C. received a postdoctoral fellowship from the French Ministry of Research.

[2] These authors contributed equally to the paper.

[3] Present address: School of Plant Biology, University of Western Australia, 35 Stirling Highway, Crawley, Western Australia 6009, Australia.

* Corresponding author; e-mail maurel@ensam.inra.fr; fax 33–4–67–52–57–37.

Article, publication date, and citation information can be found at www.plantphysiol.org/cgi/doi/10.1104/pp.105.065029.

Siefritz et al., 2002; Tournaire-Roux et al., 2003). However, in the case of roots under salt stress, the molecular and cellular mechanisms that lead to aquaporin regulation remain uncertain (Kirch et al., 2000; Martinez-Ballesta et al., 2000; Maathuis et al., 2003).

Most physiological and molecular studies on roots under salt stress addressed long-term (>12 h) responses and did not allow all the mechanisms possibly involved to be readily addressed (Azaizeh and Steudle, 1991; Carvajal et al., 1999; Martinez-Ballesta et al., 2000, 2003). Yet, the rapid regulation of individual aquaporin genes in response to salt or drought stress has been reported in several species (Yamada et al., 1995; Li et al., 2000; Kawasaki et al., 2001; Smart et al., 2001; Maurel et al., 2002). However, the high isoform multiplicity of plant aquaporins, with, for instance, 35 homologs in Arabidopsis, has rendered the significance of individual gene regulation events difficult to assess in terms of water transport regulation (Kirch et al., 2000; Suga et al., 2002). With fully sequenced plant genomes becoming available, membrane arrays that provide an extensive view of aquaporin transcriptomes can now be designed (Maathuis et al., 2003). Also, a real-time reverse transcription (RT)-PCR analysis was made possible to investigate the regulation in Arabidopsis of all 13 individual aquaporin homologs of the plasma membrane (PM) intrinsic protein (PIP) subfamily under various stress conditions (Jang et al., 2004). A note of caution is required, however, when interpreting transcriptomic data since aquaporin transcript and protein levels may not be correlated with each other, as was exemplified for developmental and environmental regulation of aquaporins in radish (Suga et al., 2001) and maize (*Zea mays*; Aroca et al., 2005). In addition, mechanisms that couple stimuli to changes in aquaporin subcellular localization can critically determine their expression properties. Such typical regulation occurs in kidney, where vasopressin stimulation triggers Aquaporin 2 expression on the apical membrane of collecting epithelial cells (Brown, 2003). Vera-Estrella et al. (2004) recently uncovered a similar mechanism in plants, showing that exposure of *Mesembryanthemum crystallinum* cells to an osmotic stress-induced redistribution of an aquaporin of the tonoplast (TP) intrinsic protein (TIP) subfamily in a putative endosomal compartment. Finally, stimulus-induced changes in aquaporin phosphorylation or protonation can play a key role in aquaporin gating under stress (Johansson et al., 1998; Guenther et al., 2003; Tournaire-Roux et al., 2003). Thus, a large variety of molecular and cellular mechanisms possibly regulate aquaporin functions under normal or stress conditions (for review, see Luu and Maurel, 2005).

In this article, we used Arabidopsis as a model to explore the short-term (≤2 h) and long-term (6–24 h) effects of salt on $L\mathrm{p_r}$ (aquaporin activity). In parallel, we investigated the expression properties of the whole complement of aquaporins. Aquaporin gene expression but also protein abundance and subcellular localization were considered. Our data establish that inhibition of water transport in response to an osmotic and not an ionic signal represents one of the earliest responses of plants to salinity. These changes are accompanied by changes in aquaporin expression at multiple levels, which may contribute to regulation of root water transport, mostly in the long term (≥6 h).

RESULTS

Hydrostatic Water Transport in the Arabidopsis Root

Hydroponically grown Arabidopsis plants were transferred to a fresh nutrient solution with or without salt concentrations up to 150 mM. After 1 h, entire root systems were excised and inserted into a pressure chamber, with a bathing solution similar to that initially applied to the intact root. All roots showed a linear relationship between exuded sap flow rate (J_v) and applied pressure (P) for 0.15 MPa $< P <$ 0.80 MPa (Fig. 1A).

P_0 was defined as the linearly extrapolated x intercept of the $J_v(P)$ curve. P_0 provides an estimate of the balancing pressure required to counteract possible osmotic driving forces present across the root. Control roots maintained in a standard nutrient solution without salt exhibited reduced spontaneous exudation and P_0 was close to zero. In salt-treated roots, P_0 was positive and increased with the strength of the saline solution, up to $P_0 = 0.4$ MPa at 150 mM NaCl. These data suggest that salt exposure results in a strong, negative osmotic pressure gradient, $\Delta\Pi_{x\rightarrow s}$, between the xylem vessels and the root bathing solution. $\Delta\Pi_{x\rightarrow s}$ can be experimentally determined from the difference in osmolality between exuded sap (Π_x) and root bathing solution (Π_s).

Figure 1B was derived from data obtained on individual roots as shown in Figure 1A. It shows that P_0 was linearly related to $\Delta\Pi_{x\rightarrow s}$, with a slope coefficient $\sigma = 0.77$ (r^2=0.89). σ can be interpreted as the root reflection coefficient, whereby $\sigma\ \Delta\Pi_{x\rightarrow s}$ represents the osmotic driving force across the root. A σ value below unity suggests that the Arabidopsis root functions as an imperfect osmometer (i.e. is somewhat permeable to solutes). This idea was corroborated by the observation that Π_x linearly increased with the externally applied salt concentration (data not shown).

Collectively, these results establish the physical basis of osmotically and hydrostatically driven water transport in the Arabidopsis root. They also show that, for plants exposed to varying salt concentrations, the slope of the $J_v(P)$ curve reported to root dry weight (DW) can be used as an estimate of $L\mathrm{p_r}$.

Effects of Salt Exposure on $L\mathrm{p_r}$

Control plants maintained in a standard nutrient solution had a mean $L\mathrm{p_r}$ value of 186.6 ± 8.8 mL g^{-1} h^{-1} MPa^{-1} ($n = 7$). Data, as exemplified in Figure 1A, indicated that treatment of plants by the same solution, but complemented with 25, 50, 100, or 150 mM NaCl, induced after 1 h a reduction in $L\mathrm{p_r}$ (in %) by

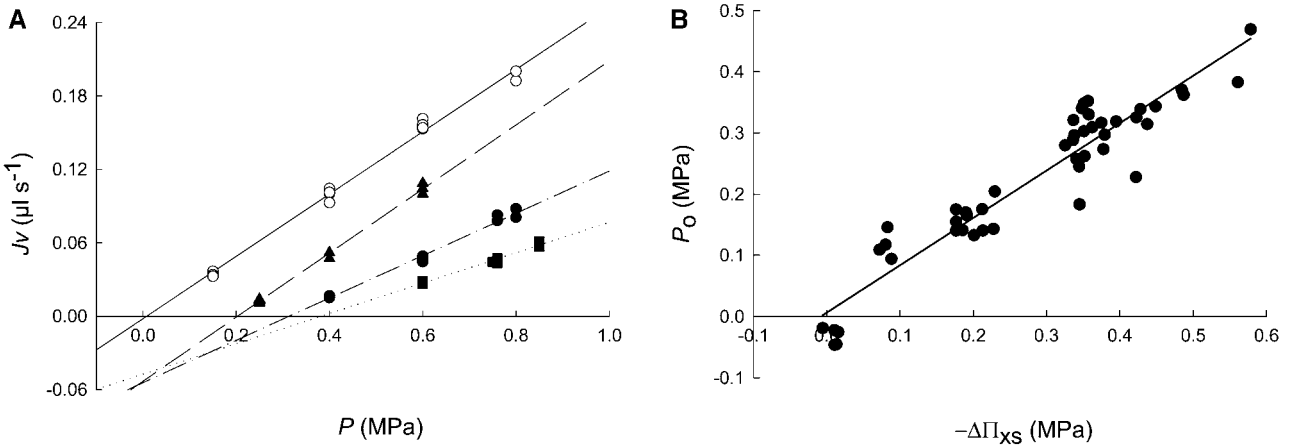

Figure 1. Pressure chamber measurements in roots of Arabidopsis plants treated with salt. A, Plants were grown for 1 h in a standard nutrient solution (○) or in a nutrient solution complemented with 50 mM NaCl (▲), 100 mM NaCl (●), or 150 mM NaCl (■). Exuded sap flow rate (J_v) was measured on excised roots at the indicated pressure (P) in the same solution as that used to treat the plants. Pressure-to-flow relationships representative of each treatment are shown. Lp_r (in mL g^{-1} h^{-1} MPa^{-1}) can be deduced from the linear fit of $J_v(P)$ curves and from the DW of corresponding root systems: ○, 148.0 ; ▲, 84.2 ; ●, 62.1 ; ■, 58.6. B, Relationship between the osmotic gradient present between xylem vessels and the root bathing solution ($\Delta\Pi_{x\rightarrow s}$) and the balancing pressure P_0. P_0 was linearly extrapolated as the x-axis intercept of individual $J_v(P)$ curves as shown in Figure 1A. For determining $\Delta\Pi_{x\rightarrow s}$, sap was collected in roots during the course of Lp_r measurements (see "Materials and Methods"). The graph presents combined data from measurements on roots from individual plants treated with a standard nutrient solution ($n = 5$) or with a nutrient solution complemented with 25 mM NaCl ($n = 4$), 50 mM NaCl ($n = 11$), 100 mM NaCl ($n = 16$), or 150 mM NaCl ($n = 16$).

21.4 ± 9.9 ($n = 8$), 46.2 ± 7.9 ($n = 6$), 61.6 ± 3.7 ($n = 7$), and 70.1 ± 4.2 ($n = 5$), respectively. Because of its marked effects on Lp_r, treatment with 100 mM NaCl was chosen as a standard salt treatment for further studies. A similar osmotic challenge, as induced by treatment with 200 mM mannitol, resulted in a similar reduction in Lp_r by 62.3 ± 5.6% ($n = 10$). This suggests that hyperosmolarity, rather than ion toxicity, is responsible for early salt-induced inhibition of Lp_r.

The kinetic effects of salt exposure on Lp_r were characterized in closer detail (Fig. 2A). In control experiments, we observed that transfer of intact plants into a different container, but containing the same standard nutrient solution, induced a significant fluctuation in Lp_r over time. In particular, Lp_r was increased by 44% from reference values after 1 h and 40 min of transfer (Fig. 2A). A similar fluctuation has been observed by Martinez-Ballesta et al. (2003) and tentatively explained as a spontaneous, diurnal variation of Lp_r. In our experiments, a similar increase in Lp_r was reproduced at whatever time of day that plant transfer was performed. In contrast to control plants, plants treated with 100 mM NaCl showed as early as 40 min after treatment a significantly reduced Lp_r with respect to control plants (Fig. 2A). Lp_r was maximally inhibited after 4 to 6 h of treatment to 25% to 30% of values in control conditions. Inhibition was maintained for 20 to 24 h of treatment. An exponential fit of these data from an average control value at initial time indicated a half-time for inhibition of $T_{1/2} = 45.3$ min (Fig. 2A).

The responsiveness of plants to salt is controlled in part by the salt overly sensitive 2 (SOS2)/SOS3 pathway (Zhu, 2003), and its possible role in salt-induced inhibition of Lp_r was investigated. Mutation of the *SOS2* gene results in a 10-fold increased sensitivity of roots to growth inhibition by salt (Zhu et al., 1998). Water transport measurements, as exemplified in Figure 1A, showed that wild-type and *sos2-1* mutant plants exhibited similar dose-dependent inhibition of Lp_r with, in both cases, 50% inhibition of Lp_r by salt concentrations between 50 and 100 mM (data not shown). In addition, treatment of *sos2-1* plants by 100 mM NaCl induced a decrease in Lp_r, down to 25% to 30% of control values, with $T_{1/2} = 31$ min (Fig. 2B). Because of the limited accuracy of $T_{1/2}$ determination, we interpret these kinetic data to mean that the Lp_r response of *sos2-1* plants to salt was qualitatively similar to that of wild-type plants. Similar to wild type, *sos2-1* plants also showed a marked inhibition of Lp_r by a 200 mM mannitol treatment (data not shown).

Macroarray Analysis of Gene Expression in the Aquaporin Family

Sequence tags specific for each of the 35 Arabidopsis aquaporin genes were searched by multiple nucleotide sequence alignments and eventually refined by pairwise comparisons. All selected tags were mostly comprised in the 3′ untranslated transcribed region, had a minimal length of 204 bp (maximum length, 361 bp), and shared less than 56% overall sequence identity with any other tag. To further reduce possible cross-hybridization (Xu et al., 2001), no conserved stretch (>80% sequence identity) greater than 22 bp was admitted, with the exception of the *PIP2;2* and *PIP2;3* tags, which shared 80% identity over a 55-bp sequence.

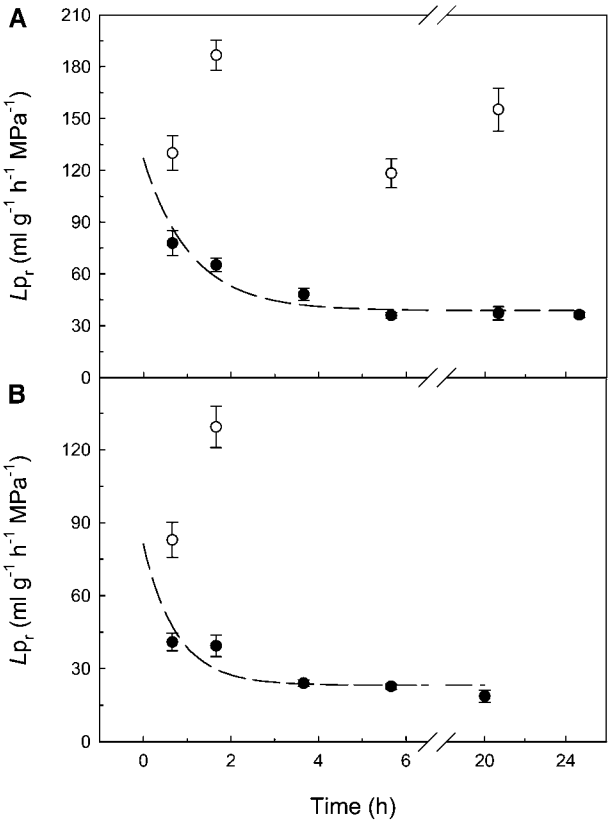

Figure 2. Kinetic changes of L_{p_r} induced by salt in wild-type (A) and *sos2-1* (B) plants. A, Wild-type plants were transferred at time 0 in a fresh standard nutrient solution (○) or in a nutrient solution complemented with 100 mM NaCl (●). Times of treatment include the 30 to 40 min required to adjust the excised root in the pressure chamber. L_{p_r} was measured as exemplified in Figure 1A. The broken line represents an exponential fit of L_{p_r} values in salt-treated plants assuming that L_{p_r} at the initial time was similar to the value measured at 1 h in untreated controls. B, Measurements on *sos2-1* plants, with the same procedure and conventions as in A.

Using these criteria, we were able to identify 32 gene-specific tags (GSTs) corresponding to 29 individual genes and three pairs of close homologs (*TIP3;1*/*TIP3;2*, *nodulin 26-like intrinsic membrane protein 1;1* [*NIP1;1*]/*NIP1;2*, and *NIP4;1*/*NIP4;2*), in which no marked divergence in sequence (<80% identity) could be distinguished.

Expression of the whole complement of aquaporin genes was followed by hybridizing macroarray membranes carrying the GSTs with a complex ^{33}P-labeled probe prepared from root cDNA (Table I). GSTs for 10 members of the PIP subfamily and five members of the TIP subfamily showed hybridization signals that were significantly above the background signal determined from negative control genes (Table I). Although these signals cannot be compared on a quantitative basis, they point to certain genes, such as *PIP1;1*, *PIP1;2*, *PIP1;3*, *PIP2;1*, *PIP2;2*, *TIP1;1*, *TIP1;2*, *TIP2;2*, and *TIP2;3*, as being highly expressed in roots (Table I). It is also noteworthy that some very close homologs of highly expressed genes showed very weak hybridization signals (compare, for instance, *PIP2;2* and *PIP2;3*, and *TIP1;2* and *TIP1;3*), suggesting that reduced cross-hybridization, if any, occurred between GSTs. In the same experiments, 14 aquaporin GSTs yielded weak, nonsignificant hybridization signals, suggesting that the corresponding genes were not or lowly expressed in roots. However, using RT-PCR, it was possible to detect transcripts for four of these genes (*PIP2;5*, *PIP2;6*, *TIP4;1*, and *NIP2;1*).

To test further the specificity of the macroarray signals, we used an Arabidopsis line with a T-DNA insertion within the *PIP2;2* gene and, therefore, a completely disrupted *PIP2;2* mRNA transcription (Javot et al., 2003). Accordingly, the *PIP2;2* signal was reduced to a basal level, whereas the hybridization signals corresponding to the other *PIP* genes were not significantly altered (Fig. 3). Altogether, these results establish that macroarrays carrying aquaporin GSTs provide reproducible and specific signals for expression profiling of individual isoforms. We also showed that a minimum of 24 aquaporin transcripts were present in roots of plants grown in standard hydroponic conditions.

Effects of Salt Exposure on Aquaporin Gene Expression

The kinetic variations of aquaporin transcript abundance in roots were studied over the first 24 h following salt treatment, with a special focus on early effects of salt until 1 h of treatment. Figure 4 represents pooled data from three independent 100 mM NaCl treatments, each being analyzed in two complete probe-labeling and hybridization experiments. Our analyses were also supported by the study of several control genes in parallel (Fig. 4, A and B). The hybridization signal of the salt-responsive *RD29B* gene was around background at initial time points (0–1 h), but rose to 2.8 times background level after 2 to 6 h of treatment (Fig. 4A). In contrast, the signals for *actin2* (*ACT2*) and *circadian clock regulated 2* (*CCR2*) transcripts showed a steady decrease over time, whereas expression of *elongation factor 1-α* (*EF1-α*) was fairly stable throughout the treatment (Fig. 4B).

Expression of *PIP* and *TIP* aquaporin genes was remarkably stable over the 2 h following salt exposure, with the exception of *PIP2;3* and *TIP2;3*, which showed a punctual increase in hybridization signal at 2 h, by 100% and 60%, respectively (Fig. 4, C and D). By contrast, a dramatic decrease in signal for the most prevalent aquaporin transcripts was observed between 2 and 4 h of treatment. Signals were maximally reduced at 6 h of treatment, by 35% (*PIP1;2*) to 65% (*PIP1;1* and *TIP2;2*). For most of these genes, expression remained low until 24 h of treatment, whereas, for a few others (*PIP1;2*, *PIP2;1*, and *TIP1;1*), a tendency for increase in signal toward initial values was observed after 24 h. By contrast, most of the lowly expressed genes (*PIP1;4*, *PIP1;5*, *PIP2;7*, and *TIP2;1*) showed a distinct pattern, with a stable signal over the first 6 h, followed in some cases by a significant decrease at 24 h (Fig. 4, C and D). Finally, no significant

Table I. *Expression level of aquaporin isoforms in roots of 30-d-old Arabidopsis plants (ecotype Col-0) grown in standard hydroponic culture conditions*

a.u., Arbitrary units; RT-PCR, no significant expression signal was measured by macroarrays, but expression could be detected by RT-PCR; n.d., expression was detectable neither by macroarrays nor by RT-PCR.

PIP[a]		TIP[a]		NIP[a]		SIP[a]	
Gene	Expression Level[b]	Gene	Expression Level[b]	Gene	Expression Level[b]	Gene	Expression Level[b]
PIP1;1	4,742 ± 472	*TIP1;1*	7,842 ± 631	*NIP1;1/2*	341 ± 135	*SIP1;1*	460 ± 107
PIP1;2	7,433 ± 1,041	*TIP1;2*	5,987 ± 439	*NIP2;1*	RT-PCR	*SIP1;2*	n.d.
PIP1;3	2,895 ± 575	*TIP1;3*	n.d.	*NIP3;1*	344 ± 118	*SIP2;1*	364 ± 87
PIP1;4	603 ± 190	*TIP2;1*	556 ± 142	*NIP4;1/2*	n.d.		
PIP1;5	863 ± 179	*TIP2;2*	7,904 ± 620	*NIP5;1*	333 ± 131		
PIP2;1	7,214 ± 1,021	*TIP2;3*	3,240 ± 270	*NIP6;1*	n.d.		
PIP2;2	14,810 ± 1816	*TIP3;1/2*	n.d.	*NIP7;1*	n.d.		
PIP2;3	873 ± 122	*TIP4;1*	RT-PCR				
PIP2;4	381 ± 106	*TIP5;1*	n.d.				
PIP2;5	RT-PCR						
PIP2;6	RT-PCR						
PIP2;7	1,735 ± 356						
PIP2;8	n.d.						

[a]Aquaporin subclass. [b]Expression level estimated by macroarray hybridization and RT-PCR. Numbers refer to hybridization signal intensities (in a.u. ± SE; $n = 12$). In these experiments, expression was statistically significant for a hybridization signal greater than the mean unspecific hybridization signal + 2 SD (315 a.u.).

change in hybridization signals for *NIP* and small basic intrinsic protein (*SIP*) genes was observed (data not shown).

To test further the specificity of salt-dependent aquaporin gene regulation, a set of 50 independently chosen Arabidopsis cDNAs was taken as a supposedly invariable reference and used to normalize the kinetic data shown in Figure 4. This procedure yielded results that were qualitatively similar to those from nonnormalized data, indicating, in particular, a significant down-regulation (25%–60%) of all abundant aquaporin transcripts after 2 h of salt treatment (data not shown).

It was also critical for the macroarray data to be validated by an independent technique. RNA samples pooled from three independent salt treatments were analyzed by northern blots, using the *PIP1;1*, *PIP2;3*, *TIP1;2*, and *TIP2;2* GSTs as probes. Although slight discrepancies were observed at certain time points (Fig. 5), these analyses qualitatively reproduced the gene expression patterns revealed by macroarrays. For instance, a marked decrease of the *PIP1;1* hybridization

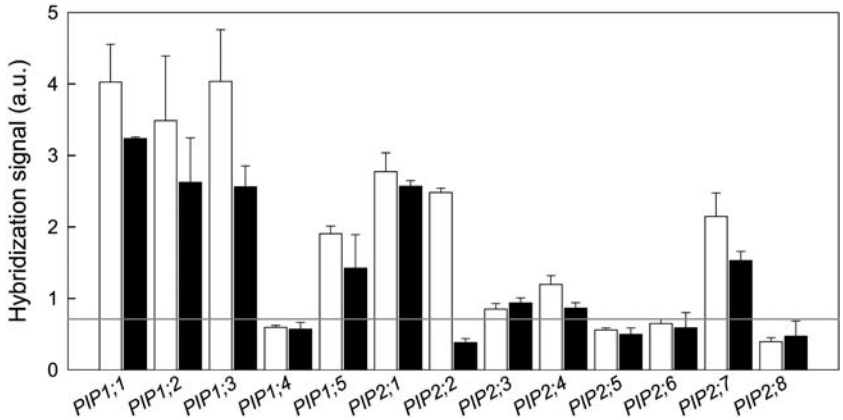

Figure 3. Expression profiling of *PIP* genes in roots of wild-type and *PIP2;2* knockout Arabidopsis (ecotype Wassilewskija) lines. Representative macroarray hybridization experiment using complex probes prepared from roots of wild-type plants (white bars) or from roots of a T-DNA insertion *PIP2;2* mutant (*pip2;2-2* line; black bars). The alterations in water transport displayed at the cell and root levels by the *pip2;2-2* mutant were described in a previous work (Javot et al., 2003). Signals (in arbitrary units, ±SD) from three independent membranes were averaged for each plant line and results from GSTs of the *PIP* subfamily only are shown. Because all manipulations were run in parallel, no normalization of the hybridization signals between the two genotypes was required for comparison. The hatched line indicates the mean level of unspecific hybridization signals + 2 SD (see description of negative controls in "Materials and Methods") and corresponds to the threshold above which a signal is considered as significantly over background. Note that GSTs for pairs of very close aquaporin homologs (*i.e. PIP1;3*/*PIP1;4* or *PIP2;2*/*PIP2;3*) yield very distinct hybridization signals, suggesting that there was no cross-hybridization.

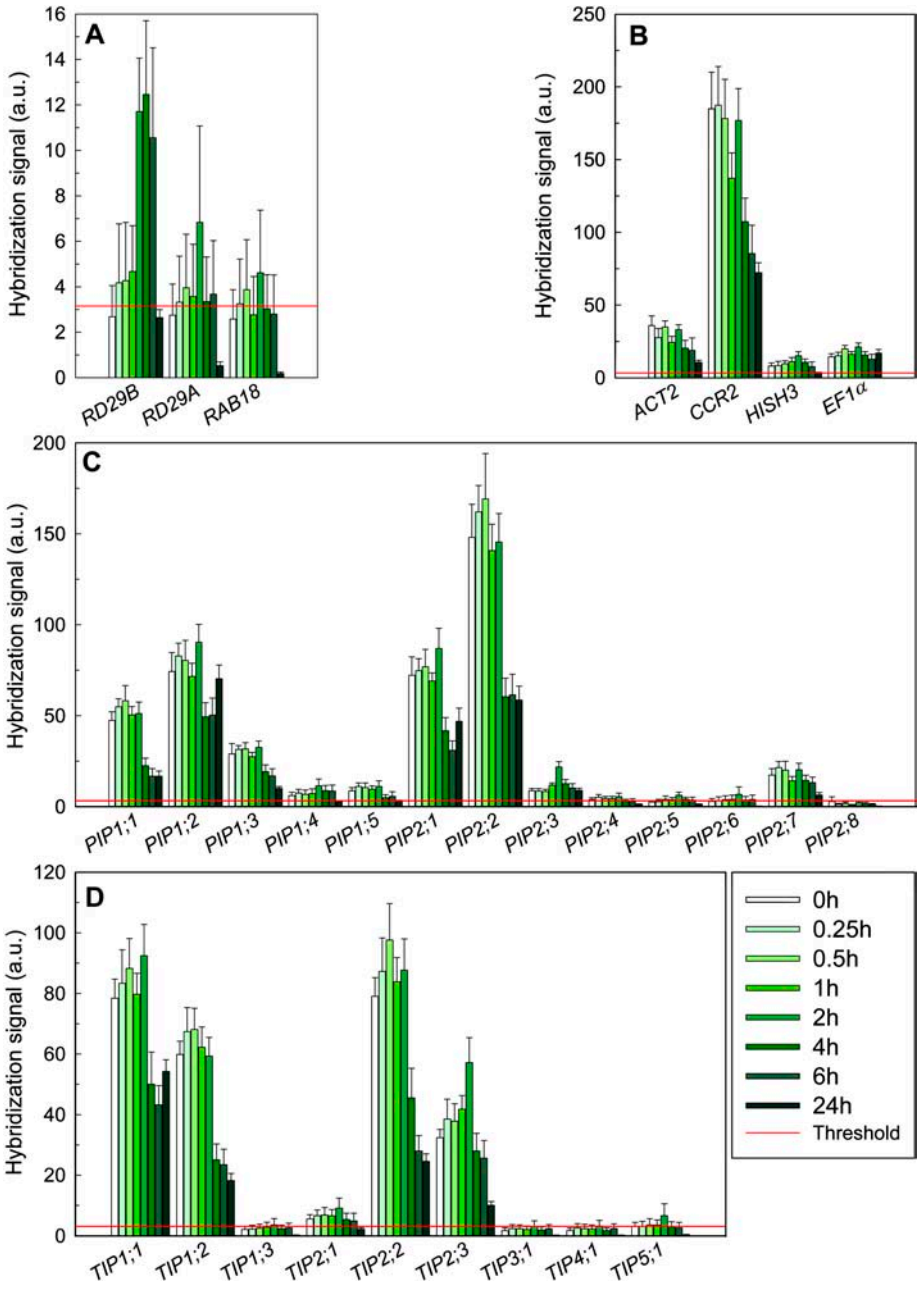

Figure 4. Kinetics of gene expression in wild-type roots treated with 100 mM NaCl. RNA was extracted from roots collected at the indicated time after treatment of plants with 100 mM NaCl. Macroarray hybridization data (in arbitrary units, ±SE; $n = 6$) were obtained from three independent salt treatments, each being analyzed in two complete probe-labeling and hybridization experiments. Data from the six individual hybridization experiments were combined, as described in "Materials and Methods," using a normalization procedure based on comparison of hybridization signals at initial time points. The red line indicates the threshold, similar in all images, above which a signal is considered as significantly over background (see Fig. 3). A, Signals from abiotic stress-regulated genes (see "Materials and Methods" for references). B, Signals from *ACT2*, *CCR2*, *histone H3*, and *EF1-α*. C, Signals from members of the *PIP* subfamily. D, Signals from members of the *TIP* subfamily.

signal was observed after 4 to 6 h of salt exposure, whereas a peak in *PIP2;3* expression was revealed at 2 h of treatment (Fig. 5).

Altogether, these results indicate a well-defined kinetic pattern of aquaporin gene expression in roots exposed to salt treatment. In particular, our study revealed that the highly expressed aquaporin genes showed coordinated reduction of expression by salt, consistent with the long-term inhibition of Lp_r.

Effects of Salt Exposure on Aquaporin Abundance

The kinetics of aquaporin expression in roots was also investigated using immunodetection methods. For this, we used antibodies raised against peptides derived from AtPIP1;1 and AtPIP2;1 (Santoni et al., 2003), and γ-VM23, a radish TIP homolog (Higuchi et al., 1998). Because of sequence conservation between aquaporin homologs, these antibodies are predicted to cross-react with several Arabidopsis isoforms of the PIP1 subfamily (PIP1;1–PIP1;4), the PIP2 subfamily (PIP2;1–PIP2;3), and the TIP1 subfamily (TIP1;1 and TIP1;2), respectively. Immunoblot analyses of total root protein extracts revealed major bands at approximately 25 (TIP1) and 50 kD (PIP1 and PIP2), consistent with detection of full-length aquaporin peptides migrating as monomeric or dimeric forms (Fig. 6A). To better resolve possible kinetic differences in abundance

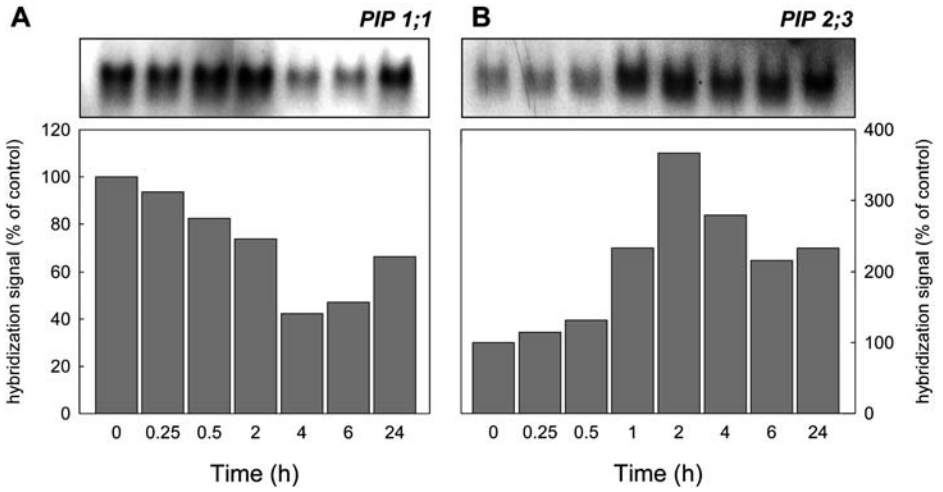

Figure 5. Northern-blot analysis of salt-dependent aquaporin gene expression in the Arabidopsis root. RNA samples extracted from roots and pooled from the three independent kinetic experiments described in Figure 4 were analyzed using the *PIP1;1* (A) or the *PIP2;3* (B) GST as a probe. The time after treatment of plants with 100 mM NaCl is indicated. For each gene, a representative autoradiograph obtained after membrane hybridization is shown (top). For each time point, the aquaporin hybridization signal was normalized with respect to a 25S rRNA hybridization signal (data not shown) and is expressed as a percentage of the aquaporin hybridization signal at the initial time (bottom). Macroarrays revealed that gene expression profiles could vary slightly between independent biological experiments. For instance, in one of three experiments, there was a clear increase in *PIP1;1* mRNA levels after 24 h. Because the combination of mRNA samples for northern blots and the combination of hybridization signals from independent macroarray experiments relied on different parameters (i.e. mRNA abundance and hybridization signal intensity, respectively), the average response may vary slightly between the two approaches. This could explain discrepancies at certain time points.

of aquaporins following exposure of roots to salinity, the extracts were also analyzed by ELISA tests. Figure 6B shows that the signal from the anti-PIP1 antibody was significantly decreased by 30% to 40% ($P < 0.05$) as soon as 30 min after salt exposure and then remained constant for up to 24 h of treatment. In contrast, the signal from the anti-PIP2 antibody was not altered after up to 6 h of treatment, but a marked drop in intensity by 40% was observed after 24 h. Similarly, the anti-TIP1 antibody yielded a signal that was fairly constant after exposure to salt, with the exception of a 24-h treatment where a slight, but significant, decrease by 20% was observed. In conclusion, the data show that PIP1, PIP2, and TIP1 aquaporins all exhibited a reduced abundance after 24 h of salt exposure, but there was no coordinated change in abundance of these three aquaporin classes in the early phase ($\leq$6 h) of the treatment.

Effects of Salt Exposure on Aquaporin Subcellular Localization

Transgenic Arabidopsis expressing a green florescent protein (GFP) fused with either the N or the C terminus of representative PIP (PIP1;1 and PIP2;1) or TIP (TIP1;1 and TIP2;1) aquaporins were observed by laser-scanning confocal microscopy.

Root cortical cells and apical cells (data not shown) of plants grown in standard hydroponic conditions revealed a consistent expression pattern of PIPs on the PM (Fig. 7, D and G) that paralleled the pattern of a GFP-low-temperature-inducible protein (LTP) fusion (Fig. 7A; Cutler et al., 2000) taken here as a reference marker for this membrane. Treatment of roots with 100 mM NaCl for 45 min altered neither the intensity of emitted fluorescence nor the subcellular staining pattern of fusions between GFP and PIP1;1 (Fig. 7E) and PIP2;1 (Fig. 7H). However, we observed after 2 h of salt treatment in a restricted number of cells (approximately 5%) the appearance of intracellular structures containing PIP1 or PIP2 homologs or LTP fused to GFP (Fig. 7, C, F, and I).

The localization in the TP of untreated control plants of fusions of TIPs with GFP was established from peripheral cell staining with intracellular invaginations that skirted the nucleus (Fig. 8, C and E) and by comparison to the pattern of AtNRAMP3-GFP (Fig. 8A), used here as a reference marker of the TP (Thomine et al., 2003). Salt treatment of TIP1;1-GFP plants induced, as early as 45 min, the labeling of small spherical intracellular bodies tentatively identified as double-membrane vacuolar invaginations (bulbs; Fig. 8D). This labeling coexisted with labeling of adjacent TP regions that delimit the overall vacuolar lumen. This pattern was consistently observed in 19 salt-treated plants and was never observed in 33 untreated plants. Bulb structures were initially described in expanding cotyledon and hypocotyl cells of Arabidopsis plantlets, but in the absence of any external stimulus (Saito et al., 2002). These structures were revealed by labeling with a TIP1;1-GFP fusion similar to the one used in this work. By contrast to TIP1;1-GFP, fusions

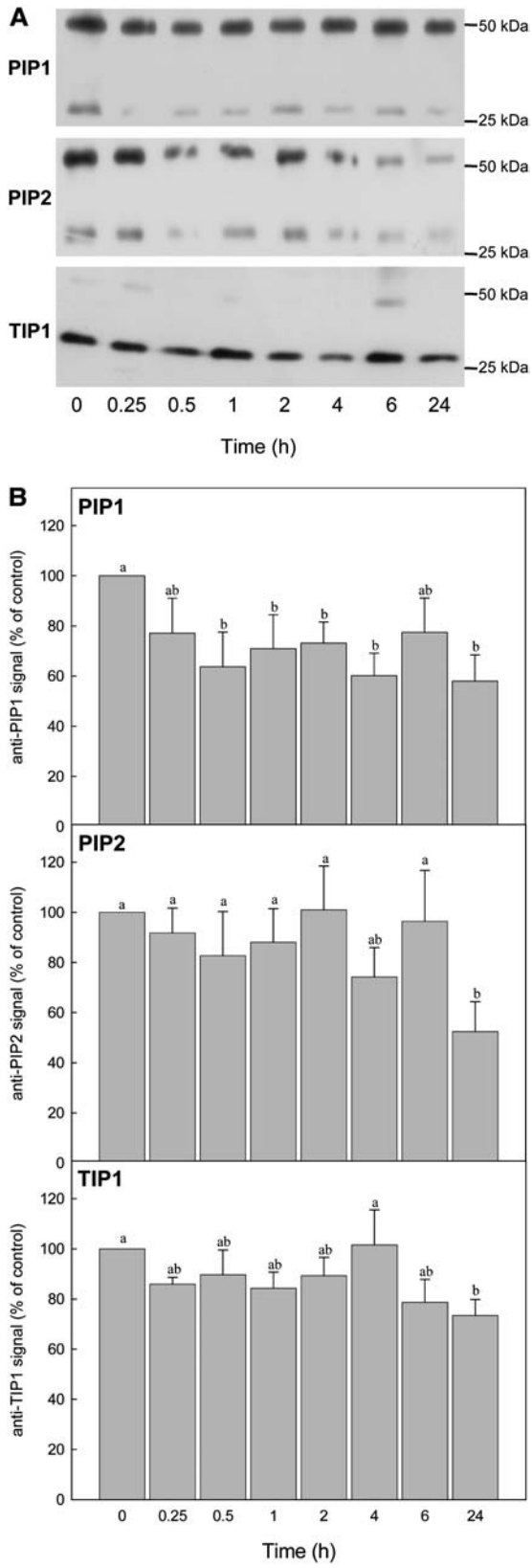

Figure 6. Time-dependent changes in aquaporin abundance in roots of salt-treated plants. A, Total proteins were extracted from roots collected at the indicated time after treatment with 100 mM NaCl. Typical western blots (5 μg protein/lane) for probing the abundance of proteins immunoreactive to an anti-PIP1 antibody (PIP1), an anti-PIP2 antibody (PIP2), or an anti-TIP1 antibody (TIP1) are shown. B, ELISA assays on total protein extracts, using the antibodies described above (same conventions). Values for each sample were compared to, and expressed as a percentage of, the control value at $t = 0$. Data (±SE, $n = 6$) from six individual ELISA assays with samples from two independent salt treatments were combined. Letters above bars indicate statistically significant ($P < 0.05$) values between time points.

between GFP and AtNRAMP3 (Fig. 8B) and TIP2;1 (Fig. 8F) did not label the bulbs, but only adjacent TP regions in salt-treated Arabidopsis roots. Overall, salt exposure had no quantitative or qualitative effect on the labeling pattern of these two TP fusion proteins.

Altogether, these data show that salt treatment can induce, although in a restricted number of cells, the partial subcellular relocalization of aquaporins in the Arabidopsis root. These effects were isoform-specific in the case of TIPs.

DISCUSSION

Biophysical Basis of Water Transport in the Arabidopsis Root

The Arabidopsis root has recently been used as a model to investigate biophysical as well as cellular and molecular aspects of water uptake (Javot et al., 2003; Martinez-Ballesta et al., 2003; Tournaire-Roux et al., 2003). In this work, we described its response to salinity. We used a physical formalism similar to that described by Munns and Passioura (1984) on intact plants, assuming that the Arabidopsis root functions as an imperfect osmometer. Interpretation of this model, however, requires some assumptions. Because of the reduced overall surface of the Arabidopsis root system, J_v can be extremely low at low driving pressures. Thus, the balancing pressure P_0 that reflects the minimal xylem tension required to support plant transpiration had to be extrapolated, assuming a linear flow-versus-force [$J_v(P)$] relationship in quasi-null flow conditions. By contrast, the composite model of root water transport (Steudle, 2000) predicts that the $J_v(P)$ curve may deviate from linearity at low pressure (for discussion, see Passioura, 1988). Here, we assumed that this deviation was negligible since, in the Arabidopsis root, the apoplastic path makes a minimal contribution and most of water transport is mediated through membranes (Martinez-Ballesta et al., 2003; Tournaire-Roux et al., 2003). In addition, the experimental $J_v(P)$ relationships determined for varying salt concentrations were remarkably linear, indicating that the osmotic behavior of the root was constant (i.e. that both Lp_r and the osmotic gradient, $\sigma\Delta\Pi_{x\rightarrow s}$) were maintained over the range of pressure examined. Although the root was somewhat permeable to salt (with a reflection coefficient σ of approximately 0.8), no external, flow-dependent accumulation of salt against cell membranes occurred within the root.

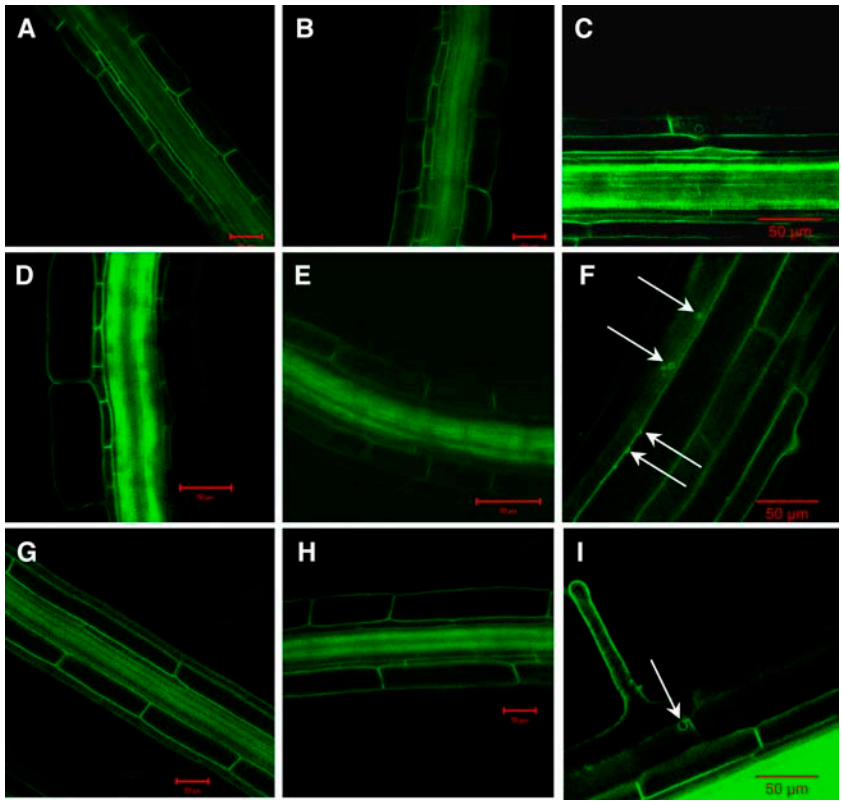

Figure 7. Effects of salinity on subcellular localization of PIPs fused to GFP. The figure shows laser-scanning confocal micrographs of the fluorescence emitted by root cells of transgenic plants grown in hydroponic culture. Observations were made 45 min after transfer of plants in a standard nutrient solution (A, D, and G), 45 min (B, E, and H), or 120 min (C, F, and I) after transfer in a nutrient solution complemented with 100 mM NaCl. Plants expressed the following fusion proteins: GFP-LTP (A–C), PIP1;1-GFP (D–F), or PIP2;1-GFP (G–I). Arrows indicate intracellular structures occasionally observed with all GFP fusion proteins after 120 min of treatment. Scale bar, 50 μm.

Stimulus-Induced Variations of Arabidopsis Lp_r

This work confirms that Arabidopsis, similar to numerous plant species (Azaizeh and Steudle, 1991; Peyrano et al., 1997; Carvajal et al., 1999; Martinez-Ballesta et al., 2000, 2003), exhibits a marked decrease in Lp_r in response to salt exposure, by ≥70% after 6 h in the presence of 100 mM NaCl. Here, we provide a description of the very early effects of salt, showing that half-inhibition of Lp_r can occur as fast as approximately 45 min.

In a previous study, Martinez-Ballesta et al. (2003) showed that mercury had differential inhibitory effects on Lp_r of Arabidopsis plants in normal and saline conditions. This was interpreted to mean that Lp_r inhibition by salt can be accounted for by down-regulation of aquaporins. This idea is corroborated by independent findings from our group showing that aquaporin contributes to >80% of Lp_r (Tournaire-Roux et al., 2003) and therefore must account for most of its salt-induced inhibition.

To complement previous studies on regulation of Lp_r under salt stress, we investigated the possible involvement of the SOS2/SOS3 signaling cascade, which plays a central role in the response of plants to salt stress. This cascade seems, however, to be specifically involved in ion homeostasis (Zhu, 2003). For instance, *sos2-1* mutant plants do not show, with respect to wild-type plants, altered sensitivity for inhibition of root growth by osmotic stress (Zhu et al., 1998). Here, we found that wild-type and *sos2-1* mutant plants exhibited a similar time and dose-dependent inhibition of Lp_r by salt. It was also found that isotonic mannitol or salt treatments had similar inhibitory effects on Lp_r of wild-type and *sos2-1* plants. Thus, Lp_r down-regulation in Arabidopsis roots is elicited by perception of an osmotic, rather than an ionic, challenge.

Surprisingly, excision of roots from control plants bathed in a standard nutrient solution and their gentle transfer in the pressure chamber induced a transient increase in apparent Lp_r. Because salt-treated roots did not show any concomitant peak increase in Lp_r, the idea that nonspecific mechanical damage of the roots induced an additional leaky hydraulic conductance can be excluded. Diurnal variations of Lp_r have been reported in several plant species, but, in our experiments, the peak increase of control root Lp_r was observed at any time of the day. Thus, we hypothesize that oxidative or mechanical stresses associated with root excision and transfer may activate Lp_r (aquaporins) by yet another signaling path that is repressed or masked under saline treatment.

A transient decrease in whole-plant water content has been shown to occur over the first 24 h of exposure of Arabidopsis plants to salt (80 mM NaCl) and was tentatively associated with changes in aquaporin gene expression (Maathuis et al., 2003). This work shows that this decrease is not correlated to Lp_r (aquaporin activity in roots), but rather reflects a transient water

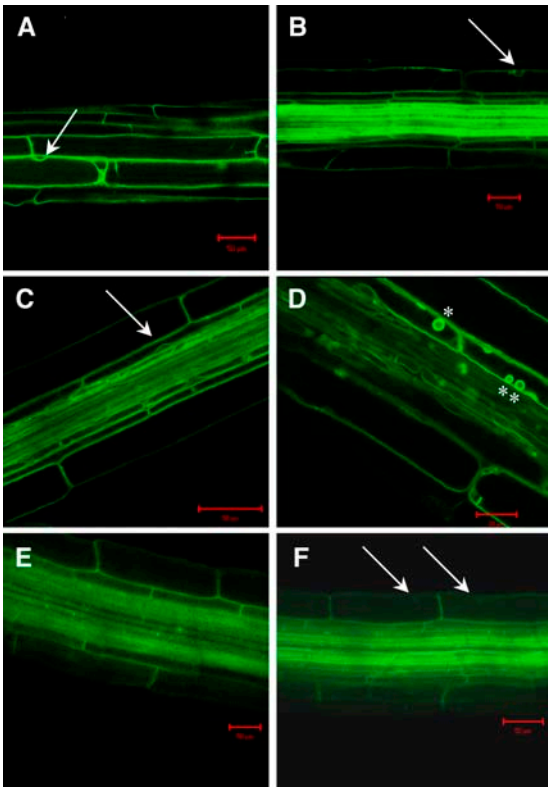

Figure 8. Effects of salinity on subcellular localization of TIPs fused to GFP. Observations were made 45 min after transfer of plants in a nutrient solution either standard (A, C, and E) or complemented with 100 mM NaCl (B, D, and F). Plants expressed the following fusion proteins: AtNRAMP3-GFP (A and B), TIP1;1-GFP (C and D), and TIP2;1-GFP (E and F). Note nuclei skirted by labeling of the TP (arrows) by AtNRAMP3-GFP (A and B), TIP1;1-GFP (C), and TIP2;1-GFP (F). Labeling of vacuolar bulbs (asterisks) is specific to salt-treated roots expressing TIP1;1-GFP (D). Scale bar, 50 μm.

imbalance of the whole plant body. Our data also suggest that, during the day, the basal permeability of Arabidopsis roots to salt may provide a path for transpiration-driven intake of salt. Down-regulation of aquaporins in roots, together with stomatal closure, could prevent the deleterious effects of excessive salt loading. Alternatively, early changes in root Lp_r may generate a hydraulic signal to trigger stomatal closure. During the night, in contrast, reduced water transport in the root may be critical to prevent a back flow of water from the plant into the soil (Steudle, 2000).

Aquaporin Gene Expression Profiling in the Arabidopsis Root

The major objective of this study was to investigate whether changes in aquaporin activity (Lp_r) are accompanied by changes in aquaporin expression. Until the recent completion of plant genome-sequencing programs, previous studies, even the most thorough, have necessarily been restricted to an incomplete number of aquaporin isoforms (Weig et al., 1997; Kirch et al., 2000; Suga et al., 2002). In this work, an aquaporin macroarray with GSTs of ≥200 bp was developed to perform gene expression profiling of the whole family in the Arabidopsis root. Here, we show that the aquaporin macroarray can distinguish between expression signals of closely related isoforms that exhibit >97% amino acid identity (i.e. *PIP1;3*/*PIP1;4*) or that have recently evolved by tandem gene duplication (i.e. *PIP2;2*/*PIP2;3*; Javot et al., 2003). Expression profiling of a *PIP2;2* knockout mutant provided additional evidence that macroarray hybridizations are highly gene specific.

For the purpose of this study, it was also crucial to obtain high-resolution kinetics of root aquaporin transcriptome. With respect to a recently published microarray analysis of aquaporin expression (Maathuis et al., 2003), the present study provides an enhanced quantification of aquaporin transcripts. Here, we confirmed that a high number of independent repetitions ($n \geq 6$) are critical to consistently resolve low-magnitude (1.5- to 2-fold) changes in hybridization signal (Pérez-Amador et al., 2001). As a result, we observed a remarkable stability of aquaporin gene expression over the first 2 h following salt treatment. This was followed by a down-regulation of all of the most abundant transcripts. Interestingly, most genes with a low expression signal had a qualitatively distinct kinetic pattern, with transcript levels being fairly stable throughout the salt treatment. The encoded isoforms may accomplish background, constitutive functions that are needed in all physiological conditions. We note that our study and that of Maathuis et al. (2003), both of which describe a coordinated down-regulation of aquaporin transcripts under salt stress, are at variance with a recent real-time RT-PCR analysis of *PIP* gene expression (Jang et al., 2004), which revealed in salt-treated roots an increase in abundance in PIP transcripts more pronounced for PIP1 genes. Young plants (2 weeks) grown under agitation in the presence of Suc were used in the latter study and this difference in plant material, with respect to the two other studies, may explain the diverging results.

A Diversity of Molecular Mechanisms That Contribute to the Short- and Long-Term Effects of Salt on Roots

The down-regulation of all prevalent PIP and TIP aquaporin transcripts after 2 h of salt treatment reflects a coordinated regulation of all aquaporin isoforms that collectively contribute to the whole root water transport capacity. Although requiring a certain delay, a decrease in aquaporin abundance occurred subsequently and was clearly measurable after 24 h of salt exposure. Altogether, these processes can provide a central mechanism for long-term, sustained reduction in Lp_r under salt stress.

We found, however, that salt-induced down-regulation of aquaporin gene expression lagged behind inhibition of Lp_r, challenging the idea that aquaporin function in plant roots under salt stress was exclusively controlled at the transcriptional level (Maathuis et al., 2003; Martinez-Ballesta et al., 2003). In

Table II. *Sequence of primers used for amplification of GSTs of aquaporin genes in Arabidopsis*

Gene	Primer[a]	Amplicon[b] Length
PIP1;1	*f*: 5′-^{819}TGTGGTTGTCATCAGAGC^{836}-3′ *r*: 5′-^{1025}GCAAATAATTCTCCTTTGGAAC^{1004}-3′	207
PIP1;2	*f*: 5′-^{839}TCCCATTCAAGTCCAGAAGCTA^{860}-3′ *r*: 5′-^{1085}AGTTGCCTGCTTGAGATAAACC^{1064}-3′	247
PIP1;3	*f*: 5′-^{804}TGCGGCTCTTTACCACCAAC^{823}-3′ *r*: 5′-^{1008}AACGATAAAACCAGATCATCCACAG^{984}-3′	205
PIP1;4	*f*: 5′-^{873}AGAAAGATTCCACGGTCCAGA^{893}-3′ *r*: 5′-^{1109}AAAACATCAATAACCGGAGCAC^{1088}-3′	237
PIP1;5	*f*: 5′-^{852}GTCCAAGACATAAAGTTTCCTACA^{875}-3′ *r*: 5′-^{1076}CACAATGTATTCTTCCATTGAC^{1055}-3′	225
PIP2;1	*f*: 5′-^{830}CTCTTGGATCATTCAGAAGTGC^{851}-3′ *r*: 5′-^{1078}CAACGCATAAGAACCTCTTTGA^{1057}-3′	249
PIP2;2	*f*: 5′-^{826}CTTGGATCCTTCAGAAGTGCAG^{847}-3′ *r*: 5′-^{1039}AGTACACAAACATTGGCATTGG^{1018}-3′	214
PIP2;3	*f*: 5′-^{826}CTCGGTTCATTCAGAAGTGCAG^{847}-3′ *r*: 5′-^{1032}CTCAATACACCAAACTTACATACG^{1009}-3′	207
PIP2;4	*f*: 5′-^{824}TTAAAGCTCTTGGCTCATTTGG^{845}-3′ *r*: 5′-^{1046}CCACATTTACAATTACACGAATGG^{1023}-3′	223
PIP2;5	*f*: 5′-^{820}ATTAAGGCGCTCGGGTCTTTC^{840}-3′ *r*: 5′-^{1039}ATTCAAAGTTGGCCCGCAAG^{1020}-3′	220
PIP2;6	*f*: 5′-^{812}CTGGTGCAATGAAGGCCTATG^{832}-3′ *r*: 5′-^{1044}TACACACAAACCTCCCCCACA^{1024}-3′	233
PIP2;7	*f*: 5′-^{828}CAACGCAACCAATTAATGAAGG^{849}-3′ *r*: 5′-^{1130}TTGAAGGATCTTGTGATGTTGTG^{1108}-3′	303
PIP2;8	*f*: 5′-^{822}CAACCCAACCAATTGATGATTC^{843}-3′ *r*: 5′-^{1066}GCATGGGGGTTCATATAAACTTG^{1044}-3′	245
TIP1;1	*f*: 5′-^{736}CTCCCAACCACAGACTACTGAA^{757}-3′ *r*: 5′-^{994}GGCAAAAAGAGATATTGCAACACTTG^{969}-3′	259
TIP1;2	*f*: 5′-^{740}AATTGCCTACCACCGATTACTG^{761}-3′ *r*: 5′-^{949}TACAATTGCACAAAAGCCTTCC^{928}-3′	210
TIP1;3	*f*: 5′-^{5}CTATCAACAGAATTGCGATTGG^{26}-3′ *r*: 5′-^{238}AAACGTTAGCTCCAACGGAAAC^{217}-3′	234
TIP2;1	*f*: 5′-^{723}ACATGTTCCTCTTGCTTCTGCT^{744}-3′ *r*: 5′-^{1083}TGACGATGATCTCGAAACTTCT^{1062}-3′	361
TIP2;2	*f*: 5′-^{726}AGCTCCCACCACAGAAAGCTA^{746}-3′ *r*: 5′-^{948}GCCATTAACACATGCAAGAAAG^{927}-3′	223
TIP2;3	*f*: 5′-^{737}GTGAGATCCGAGTGTAATTGACTG^{760}-3′ *r*: 5′-^{940}GAAAGAAACCAAACATGCTATACG^{917}-3′	204
TIP3;1/TIP3;2	*f*: 5′-$^{76/76}$ACTTTAGCTGAGTTTCTTTCCAC$^{98/98}$-3′ *r*: 5′-$^{388/388}$TCAACAAGAGACAAGCGAGGAT$^{367/367}$-3′	313
TIP4;1	*f*: 5′-$^{-7}$AAAAGCCATGAAGAAGATCGAG^{15}-3′ *r*: 5′-^{208}CAGATATCATTACCGCCACAAC^{187}-3′	215
TIP5;1	*f*: 5′-^{3}GAGAAGAATGATTCCAACATCG^{24}-3′ *r*: 5′-^{262}GATTCACATGACCACCAGAGAC^{241}-3′	260
NIP1;1/NIP1;2	*f*: 5′-$^{603/594}$TAATAGAGCGATCGGAGAACTTG$^{625/616}$-3′ *r*: 5′-$^{857/848}$GAACCACTTTTAGTTATTTCTCG$^{835/826}$-3′	255
NIP2;1	*f*: 5′-^{11}TATCAGTGAGCAAAAGCAACCA^{32}-3′ *r*: 5′-^{269}ACTATACCCCAAACCACAGCAA^{248}-3′	259
NIP3;1	*f*: 5′-^{600}GACTTATGGTTTGTTACGATCGAC^{623}-3′ *r*: 5′-^{822}CATCGATATAATTCACGCCAA^{802}-3′	223
NIP4;1/NIP4;2	*f*: 5′-$^{62/62}$GCAAAGATAGCCAAGGAGGAAT$^{83/83}$-3′ *r*: 5′-$^{294/294}$ACCGGAAATGTGACCAGTAGAG$^{273/273}$-3′	233
NIP5;1	*f*: 5′-^{722}CATCGACTGGTGGATCTATGAA^{743}-3′ *r*: 5′-^{1024}CATCGCCTTTTATTCTTCACAC^{1003}-3′	303
NIP6;1	*f*: 5′-^{741}TTCGATGAACCCTGTAAGAACA^{761}-3′ *r*: 5′-^{1002}TTATAAGCATCGTCGACTTCAGA^{980}-3′	262
NIP7;1	*f*: 5′-^{740}TCGGAGTTTTGACATACAGATCA^{762}-3′ *r*: 5′-^{992}CCCTGTTTTCATTTGCTTTACC^{971}-3′	253
SIP1;1	*f*: 5′-^{637}TTCGTAGGAGCATTATCTGCTG^{658}-3′ *r*: 5′-^{943}AAACCGGAAGAGAGTCTGAATG^{922}-3′	307

(*Table continues on following page.*)

Table II. (*Continued from previous page.*)

Gene	Primer[a]	Amplicon[b] Length
SIP1;2	*f*: 5′-^{681}AATTATATTTCCGGCTCCACCT^{702}-3′ *r*: 5′-^{898}TTACGCACTAACCGAGAAAATG^{877}-3′	218
SIP2;1	*f*: 5′-^{599}TACTTGTGTATTGGCTTGGACCT^{621}-3′ *r*: 5′-^{911}TCATATTGCGCATTGGACTTAC^{890}-3′	313

[a]*f*, Forward primer; *r*, reverse primer. The numbers on each primer, which are doubled in the case of a gene pair, indicate the position of the nucleotide sequence from the initial ATG codon. [b]Expected length of amplicon according to predicted cDNA sequence (http://www.tigr.org/).

these respects, a significant decrease in the abundance of PIP1 proteins was observed in whole-cell extracts as soon as 30 min after salt exposure (Fig. 6A). This points to a rapid response to salt through dynamic control of PIP1 aquaporin translation and/or degradation, the significance of which remains unclear at the moment.

Functional interactions between isoforms of the PIP1 and PIP2 subclasses have been suggested through genetic studies in planta (Martre et al., 2002) and further demonstrated after heterologous expression in Xenopus oocytes (Fetter et al., 2004). Thus, down-regulation of PIP1s in salt-treated roots might have interfered with the function of PIP2s through an altered subcellular localization of aquaporins of either subclass. In addition, stimulus-dependent trafficking of aquaporins between the PM and intracellular compartments (Barkla et al., 1999; Kirch et al., 2000; Vera-Estrella et al., 2004) may provide an efficient mechanism for rapid inhibition of L_{pr}. These ideas prompted us to study the effects of saline treatment on the subcellular localization of representative members of both the PIP1 and PIP2 subclasses. Although providing semiquantitative data, the use of transgenic plants expressing individual PIPs fused to GFP suggested that both the abundance and the subcellular localization of the fusion proteins were unchanged during the early phase (45 min) of salt treatment. In a longer term (2 h), a few intracellular structures containing PIPs and another PM marker (LTP-GFP) were observed in root cortical cells. Although the nature of these structures needs to be characterized in greater detail, their occurrence points to a general internalization mechanism that may contribute to reducing the abundance of PIPs at the PM of salt-stressed root cells.

The gating of PIPs by intracellular protons provides a mechanism for coordinated inhibition of PIPs in roots under anoxic stress (Tournaire-Roux et al., 2003). Salt has been reported to induce a cytosolic acidosis in certain algae (Katsuhara et al., 1989). However, measurements in excised Arabidopsis roots, by means of in vivo ^{31}P-NMR (R. Bligny and C. Maurel, unpublished data), or in root hairs with a pH-sensitive microelectrode (Halperin et al., 2003) failed to reveal any salt-induced change in cytosolic pH. Therefore, salt must exert its early effects on L_{pr} through a posttranscriptional mechanism different from that involved in anoxia. Protein phosphorylation might be such a mechanism, since we know that PIP aquaporins can be phosphorylated in the Arabidopsis root (Santoni et al., 2003). This modification mediates aquaporin regulation under water stress in soybean (*Glycine max*) root nodules and spinach (*Spinacia oleracea*) leaves (Maurel et al., 1995; Johansson et al., 1998; Guenther et al., 2003) and during recovery from chilling in a tolerant maize cultivar (Aroca et al., 2005).

Whereas the role of PIPs in root water uptake is now well established (Siefritz et al., 2002; Tournaire-Roux et al., 2003), our work also revealed very significant salt-dependent regulatory mechanisms for TIPs. At the gene level, and to a lesser extent at the protein level, expression of TIPs and PIPs was coordinately reduced. This could mean that TIPs also contribute to control transcellular water transport in roots. Alternatively, coregulation of PIPs and TIPs could reflect the necessity for plant cells to control under all conditions the water permeability of the vacuole and PM and, therefore, is a feature critical for cellular water homeostasis (Maurel et al., 2002). Salt exposure also induced a striking relocalization of a TIP1;1-GFP fusion in bulbs tentatively identified as vacuolar invaginations. These structures have been described in detail by Saito et al. (2002) in developing cotyledons of Arabidopsis, where they can be labeled by a TIP1;1-GFP but not by GFP-AtRab75c, another classic TP marker. Here, we showed that, in salt-treated root cells, the labeling of bulbs is specific to certain aquaporin isoforms since a TIP2;1-GFP fusion remained exclusively localized in the peripheral TP domains of central vacuoles. Significant expression of TIP1;1 was also present in these domains, suggesting that the relocalization of this aquaporin in bulbs must have reduced effects on the overall TP hydraulic conductivity. We rather believe that the bulbs correspond to vacuolar membrane domains specialized in TIP1;1 compartmentalization for further degradation of this isoform. Alternatively, the bulbs may unravel a rapid salt-induced reshaping of the root cell vacuolar apparatus with, possibly, the formation of a new vacuolar subtype.

In conclusion, this work demonstrates that exposure of plant roots to salt results in a variety of effects on L_{pr} (aquaporin activity), but also on the abundance of aquaporin mRNAs and proteins and on their subcellular localization. Kinetic measurements were critical to unravel the occurrence of posttranscriptional regulation processes during the early response of roots, whereas long-term regulation of L_{pr} can mostly

be accounted for by aquaporin transcriptional regulation. Thus, several mechanisms may work in combination and contribute to the sustained inhibition of L_{p_r} during salt stress. Altogether, these results also establish the regulation of Arabidopsis root aquaporins by salt as a unique model for studying the role of osmotic cell signaling in plant-water relations.

MATERIALS AND METHODS

Plant Materials and Growth Conditions

For determining the specificity of macroarray hybridizations, we used Arabidopsis (*Arabidopsis thaliana* ecotype Wassilewskija) plants that were either wild type or carried an *Agrobacterium tumefaciens*-transferred DNA insertion within the *PIP2;2* gene (*pip2;2-2* line; Javot et al., 2003). The effects of salt were characterized in wild-type and *sos2-1* Arabidopsis (ecotype Columbia [Col-0]). Seedlings were cultured in vitro for 10 d and further transplanted into hydroponic culture as previously described (Javot et al., 2003). Briefly, plantlets were mounted on 30- × 30- × 1.8-cm polystyrene rafts (9–15 plants per raft) floating in a basin with 8 L of aerated culture solution [1.25 mM KNO_3, 0.75 mM $MgSO_4$, 1.5 mM $Ca(NO_3)_2$, 0.5 mM KH_2PO_4, 50 μM FeEDTA, 50 μM H_3BO_3, 12 μM $MnSO_4$, 0.7 μM $CuSO_4$, 1 μM $ZnSO_4$, 0.24 μM MoO_4Na_2, 100 μM Na_2SiO_3) and grown in a growth chamber at 70% relative humidity with cycles of 16 h of light (180 μE m^{-2} s^{-1}) at 22°C and 8 h of dark at 21°C. Culture solution was replaced weekly. For gene expression analyses, the nutrient solution was complemented or not by 100 mM NaCl at day 20 after transfer in hydroponics. Treatments of various durations, as indicated in the text, were administered sequentially in order to collect all plant materials within 20 min, starting 11 h after the onset of the subjective day period. Thus, possible diurnal fluctuations of aquaporin gene expression could be excluded from kinetic analyses of salt effects. Plant material corresponding to the same time point was harvested in less than 1 min and stored at −80°C prior to RNA isolation. For water transport assays and for microscopic observations, plants were used 20 to 25 d after transfer in hydroponic culture at any time of the subjective day.

Measurement of L_{p_r}

Measurements were performed essentially as described by Javot et al. (2003) and Tournaire-Roux et al. (2003). Briefly, the root system of a freshly detopped Arabidopsis plant was inserted into a pressure chamber filled with the same nutrient solution as applied to the intact root. The hypocotyl was carefully threaded through the soft plastic washer of the metal lid and connected to a dry 50-μL glass micropipette using a low-viscosity dental paste (President Light; Coltene). Pressure was then slowly applied to the chamber, using nitrogen gas, and the rate of exuded sap flow was determined over successive 5- to 20-min periods for stabilized hydrostatic pressures between 0.15 and 0.8 MPa. The exuded sap filling the micropipette was collected, and, at the end of the measurement series, the root system was removed and root DW was measured. The hydraulic conductivity of an individual root system (L_{p_r}; in mL g^{-1} h^{-1} MPa^{-1}) was calculated from the slope of a plot, rate of flow versus driving pressure, divided by the DW of the root system. The osmolality of exuded sap was measured by freezing-point depression osmometry.

Total RNA Isolation

One to 2 g of frozen roots were ground under liquid nitrogen, resuspended in 10 mL of homogenization buffer (4 M guanidine thiocyanate, 100 mM NaCl, 10 mM EDTA, 7 mM β-mercaptoethanol, 0.5% IGEPAL CA-630, 25 mM Tris-Cl, pH 7.6), incubated for 5 min at 60°C, and centrifuged at 10,000*g* for 10 min at 4°C. The supernatant was extracted twice with phenol:chloroform:isoamyl alcohol (25:24:1; v/v/v), once with chloroform:isoamyl alcohol (100:1; v/v), and then precipitated with an equal volume of isopropanol in the presence of 0.3 M sodium acetate. The subsequent pellet was resuspended in 3 mL diethylpyrocarbonate-treated water, cleared for insoluble materials, and precipitated again overnight at 4°C in the presence of 2 M LiCl and 0.5 mM $MgCl_2$. Total RNA was recovered by centrifugation at 10,000*g* for 30 min at 4°C, washed with 70% (v/v) ethanol twice, resuspended in diethylpyrocarbonate-treated water, quantified by optical density measurements at 260 nm, and stored at −80°C until use.

Identification of Aquaporin GSTs

Sequence analyses were essentially based on existing Arabidopsis aquaporin gene annotations (Johanson et al., 2001; Quigley et al., 2001). For each aquaporin gene, we considered the DNA sequence encompassing the putative coding sequence surrounded by up to 200 and 300 bp of the 5′ and 3′ untranslated transcribed regions, respectively. Where possible, these regions were more specifically delimited on the basis of published cDNA sequences and putative polyadenylation signals. To identify transcribed GSTs of >200 bp, the 35 aquaporin gene sequences were aligned using the ClustalW and Lfasta programs. Sequences as close as possible to the 3′ end of the expressed sequence were preferred. Candidate GSTs were further tested by pairwise alignments using an Lfasta program to ensure that the maximum identity between selected aquaporin sequences did not exceed 80% in a >22-bp overlapping region and 85% in a 10- to 20-bp overlapping region (Xu et al., 2001). The specificity of the GSTs was also examined using BLAST analyses against the entire Arabidopsis genome. GSTs were more specifically defined to be bordered by gene-specific 18- to 26-bp primers with a melting temperature between 50°C and 60°C. The sequences of primers used for amplification of GSTs are provided in Table II.

GST Cloning, Amplification, and Arraying

All GSTs were amplified by RT-PCR amplification, using, if not specified, cDNA from an Arabidopsis cell suspension (Gerbeau et al., 2002). GSTs specific for *SIP2;1*, *NIP4;1*, *TIP2;1*, *TIP2;3*, *TIP3;1*, *TIP3;2*, and *TIP4;1* failed to be amplified from this material and were obtained from Arabidopsis seedling cDNA. A fragment specific for *SIP1;2* was obtained from expressed sequence tag clone RZ107g09 (Kazusa DNA Research Institute; Asamizu et al., 2000). Consequently, none of the 32 aquaporin GSTs was amplified from genomic DNA.

For all amplifications, we used a touchdown PCR method with an annealing temperature reduced over eight cycles from 62°C to 55°C, and stabilized at 55°C over the 30 subsequent cycles. The amplified aquaporin sequences were cloned into the *Eco*RV site of pBluescript II KS (+) (Stratagene). All recombinant plasmids were sequenced to check the validity of the amplified GST. The aquaporin target DNA to be spotted was amplified by PCR from 1 ng each of the plasmids described above, using primer KS17 (5′-CGA GGT CGA CGG TAT CG-3′) and SK21 (5′-CCG CTC TAG AAC TAG TGG ATC-3′). These primers, which annealed at −11 bp and +22 bp away from the *Eco*RV cloning site of pBluescript II KS (+), respectively, were selected to reduce the amount of amplified linker sequences. All PCR products were extracted with chloroform, precipitated with ethanol, and then washed twice with 70% ethanol. PCR products were checked by agarose gel electrophoresis, quantified by optical density measurements at 260 nm, and resuspended at a final concentration of 0.5 mg mL^{-1}. To check the specificity and sensitivity of hybridization signals, and also standardize the data after hybridization, control cDNA fragments were also arrayed on the membrane. Positive controls included genes known to be expressed in Arabidopsis, such as *ACT2* (Desprez et al., 1998), *CCR2* (Carpenter et al., 1994), *histone H3*, and *EF1-α* (Bernard et al., 1996). Negative controls included the cDNAs of human nebulin, desmin, DNA of an empty pBluescript II KS (+) vector, and sonicated fish sperm DNA (Bernard et al., 1996). We also included cDNA fragments from four abiotic stress-regulated genes such as abscisic acid- and drought-responsive *RAB18* and *AtDI21* (Gosti et al., 1995), and water-stress-responsive *RD29A* and *RD29B* (Yamaguchi-Shinozaki and Shinozaki, 1993). In total, duplicates of 57 samples, including 32 aquaporin GSTs and various controls, were deposited onto 3.5- × 5.5-cm Appligene positive nylon membranes using a robotic arrayer (BioGrid; BioRobotics) with five hits on each spot (approximately 100 ng DNA/spot). After denaturation for 2 × 10 min in 1.5 M NaCl, 0.5 M NaOH, and neutralization for 2 × 10 min in 1.5 M NaCl, 1 M Tris-Cl, pH 7.4, DNA samples were air dried at 80°C for 2 h and cross-linked by UV radiation at 230 nm for 75 s. Membranes were conserved at room temperature until use.

Radiolabeled Probe Synthesis

Total RNA (30 μg) was incubated for 1 h at 42°C in the presence of 8 μg oligo(dT)25, 1 mM dATP, 1 mM dTTP, 1 mM dGTP, 40 μCi [α-^{33}P]-dCTP, 10 mM dithiothreitol, 400 units SuperScript II (Life Technologies), or 800 units RT-*Moloney murine leukemia virus* (Promega) in its running buffer, in a total volume of 30 μL. The RNA template was then hydrolyzed in the presence of 0.3 N NaOH for 30 min at 65°C. The mixture was then neutralized with 0.2 N HCl, 0.3 M Tris-Cl, pH 8.3, ethanol precipitated in the presence of 1 mg mL^{-1}

sonicated fish sperm DNA or purified on a Sephacryl 100 column. Incorporation of [α-^{33}P]-dCTP was determined by scintillation counting. After denaturation for 5 min at 95°C in the presence of 5 μg oligo A80, the probe was used for hybridization at a final concentration of 1.5 to 2.0 $\times$ 10^6 cpm mL^{-1}.

Hybridization Procedures and Data Analysis

Membranes were hybridized overnight at 48°C in a hybridization buffer (50% formamide, 8% dextran sulfate, 4× SSC, 10× Denhardt, 0.5% SDS, 1 mM EDTA, 100 μg mL^{-1} denatured sonicated fish sperm DNA, 50 mM NaH_2PO_4, pH 7.2) containing cDNA complex probes labeled as described above. Membranes were then washed at 48°C, successively for 2 $\times$ 15 min in 2× SSC, 0.1% SDS, for 15 min in 1× SSC, 0.1% SDS, and for 2 $\times$ 15 min in 0.1× SSC, 0.1% SDS. To evaluate the homogeneity of target DNA spotting, membranes were subsequently hybridized to a ^{33}P-labeled oligonucleotide probe BS20 (5′-ATCGAATTCCTGCAGCCCGG-3′). This 20-bp sequence located in the amplified vector linker is common to all target DNA fragments. Filters were hybridized at 48°C to ^{33}P-BS20 in a solution containing 6× SSC, 0.5% SDS, 5× Denhardt, and 20 μg mL^{-1} denatured sonicated fish sperm DNA. After hybridization, membranes were washed as described above, except that the last wash was at room temperature. Membranes were exposed to the imaging plate of a Kodak storage phosphor screen GP (Eastman-Kodak) or a Fuji BAS-MS 3543 (Fuji Photo Film) for varying periods. Hybridization signals were captured using a Storm 840 PhosphorImager (Molecular Dynamics) with a resolution of 50 μm. Identification and quantification of the hybridization signals, as well as the subtraction of local background values, were carried out using ImageMaster array 3.01c (Amersham-Pharmacia Biotech). For each membrane spot, the signal intensity of hybridization to a complex probe (I_{cDNA}) was reported to the signal intensity of hybridization to the BS20 oligonucleotide probe (I_{oligo}), yielding a normalized signal $I = I_{cDNA}/I_{oligo}$. Background signal (I_{neg}) was calculated as the mean signal from all negative control genes. A hybridization signal was considered as significantly over background for $I > I_{neg} + 2$ SD. For each individual kinetic experiment, manipulations corresponding to all time points (i.e. mRNA extraction, cDNA labeling, membrane hybridization, and exposure to PhosphorImager) were run in parallel. This provided a high reproducibility between independent membranes for a given time point and high consistency between distinct time points. We also used a set of 50 independently chosen Arabidopsis cDNAs as a supposedly invariable reference for comparison of data between time points. In practice, a correction factor between two time points was deduced from a linear regression on a log-log representation of hybridization signals of the reference cDNAs in the two time points. For comparison of two independent kinetic experiments, we determined a normalization factor based on comparison of initial time points of the two experiments. This factor was deduced from a linear regression on a log-log representation of hybridization signals of all aquaporins in the two initial time points. The factor was then converted for a linear representation of data and used to normalize all time points of the same kinetic experiment.

Extraction of Total Proteins from Arabidopsis Root

Roots (0.4–0.8 g fresh weight [FW]) were harvested from Arabidopsis plants grown in a nutrient solution as indicated and ground in liquid nitrogen. The resulting powder was incubated with 1 mL of 10% trichloroacetic acid, 0.07% β-mercaptoethanol in acetone for 30 min at −20°C, and centrifuged at 4°C for 10 min at 40,000*g*. The pellet was washed twice with acetone, 0.07% β-mercaptoethanol, and resuspended in 1 mL/mg FW of a lysis buffer (9 M urea, 4% CHAPS, 0.5% Triton X-100, 65 mM dithiothreitol). After 30 min under agitation, the extract was centrifuged for 10 min at 10,000*g* and the supernatant containing total proteins recovered. Protein concentrations were measured using a modified Bradford procedure (Santoni et al., 2003).

Immunodetection Methods for Aquaporin Quantification in Total Protein Extracts

Antibodies were raised in rabbit against a 42-amino acid N-terminal peptide of AtPIP1;1, a 17-amino acid C-terminal peptide of AtPIP2;1 (Santoni et al., 2003), or a 14-amino acid C-terminal peptide of VM23, a radish (*Raphanus sativus*) TIP1 homolog (Higuchi et al., 1998). Western blotting was performed as described (Santoni et al., 2003). For ELISA assays, serial 2-fold dilutions in a carbonate buffer (0.03 M Na_2CO_3, 0.06 M $NaHCO_3$, pH 9.5) of 2.4 μg of total protein extracts were loaded in duplicate on immunoplates (Maxisorp). After overnight incubation at 4°C, the plates were rinsed once with phosphate-buffered saline (PBS; 137 mM NaCl, 2.7 mM KCl, 10 mM Na_2HPO_4, 2 mM KH_2PO_4, pH 7.4) and incubated for 1 h with PBS-TB (PBS plus 0.1% Tween 20, 1% bovine serum albumin) at 37°C. The plates were then rinsed three times with PBS-T (PBS, 0.1% Tween 20) and incubated with a 1:2,000 dilution of a primary antiaquaporin antibody. After 2 h at 37°C, the plates were washed five times with PBS-T and further incubated for 2 h at 37°C in the presence of a 1:2,500 dilution of a secondary peroxidase-coupled anti-rabbit antibody. After five washes in PBS, a peroxidase reaction was initiated by addition of 0.23 mM diammonium 2,2′-azino-bis-3-ethylbenzothiazoline-6-sulfonate, 0.1 M citric acid, 0.03% H_2O_2, pH 4.35. A linear regression between the absorbance signal as read with a multiplate reader (Victor; Perkin-Elmer) and the amount of total proteins was obtained for each sample and used for relative comparison between samples.

Fusion of Aquaporin and GFP cDNAs and Expression in Transgenic Plants

All constructs were made using Gateway cloning technology (Invitrogen) according to the manufacturer's instructions. The cDNAs of all 35 Arabidopsis aquaporins were PCR amplified with primers allowing the addition of *attB* recombination sites and cloned into a pDONR 207 vector using a Gateway BP Clonase enzyme mix (Invitrogen). The cDNAs were then transferred into the binary destination vectors pGWB5 and pGWB6 (Dr. Nakagawa, Shimane University, Matsue, Japan) by using a Gateway LR Clonase enzyme mix (Invitrogen). The pGWB5 and pGWB6 vectors allow fusion of GFP with the aquaporin C terminus (AQP-GFP) or N terminus (GFP-AQP), respectively, and expression of the resulting cDNA is placed under the control of a cauliflower mosaic virus 35S promoter and of the 3′ untranslated transcribed region of a *NOS* gene. All constructs were checked by DNA sequencing (Genome-Express). *A. tumefaciens* strain GV3101 (pMP90) was transformed with the pGWB constructs selected for rifampicin (50 mg L^{-1}) and kanamycin (50 mg L^{-1}) resistance, and used for transformation of Arabidopsis Col-0 by the floral-dip method (Clough and Bent, 1998). To select for transformed plants, seeds were surface sterilized and germinated on cleared polystyrene culture boxes (12 $\times$ 12 cm) containing a half-strength Murashige and Skoog medium (Murashige and Skoog, 1962) complemented with 7 g L^{-1} agar, 40 mg L^{-1} hygromycin, pH 6, in a controlled environment at 24°C under 16 h of light/d (50–100 μE m^{-2} s^{-1}). After 7 to 10 d, hygromycin-resistant seedlings were transplanted into potting soil and grown to maturity. Plants containing the following constructs, PIP1;1-GFP, PIP1;2-GFP, GFP-PIP2;1, PIP2;1-GFP, GFP-TIP1;1, and TIP1;1-GFP were obtained using the procedure in this work. Transgenics plants expressing GFP-PIP1;2, GFP-PIP2;1, and GFP-TIP2;1 were those described by Cutler et al. (2000).

Microscopic Observations of Transgenic Plants

Transgenic Arabidopsis plantlets grown on half-strength Murashige and Skoog medium without any antibiotic selection were screened for GFP expression using an Olympus BX610 microscope equipped with an epifluorescence condenser and a fluorescein isothiocyanate/enhanced GFP/bodypy/fluo3 filter set. Observations of transgenic root cells treated or not with salt were conducted on hydroponically grown plants with an inverted confocal laser-scanning microscope (Zeiss LSM 510 AX70). The argon laser excitation wavelength was 488 nm; GFP emission was detected with the filter set for fluorescein isothiocyanate (BP 500 to 530). Plants were transferred into a nutrient solution complemented or not by 100 mM NaCl and the GFP signal was examined after 45 or 120 min of treatment on a sample of root tissue under a glass coverslip. Transgenic plants expressing a GFP-LTP fusion (Cutler et al., 2000) or a NRAMP3-GFP (Thomine et al., 2003) were used as references for GFP signal localization in the PM and TP, respectively. Depending on treatments and genotypes, the number of individual plants analyzed was between 4 and 33.

Sequence data from this article can be found in the GenBank/EMBL data libraries under accession numbers as described by Johanson et al. (2001).

ACKNOWLEDGMENTS

We are grateful to Dr. Gosti and Dr. Doumas (Biochimie et Physiologie Moléculaire des Plantes, Montpellier, France) for their helpful advice on macroarray techniques. We also thank Dr. Lurin and Dr. Small (Unité de

Recherche en Génomique Végétale, Evry, France) for cloning aquaporin cDNAs in pDONR 207, Dr. Nakagawa (Shimane University, Matsue, Japan) for the gift of pGWB vectors, Gaëlle Viennois (Biochimie et Physiologie Moléculaire des Plantes, Montpellier, France) for skillful assistance in microscopic observations, and Dr. Santoni and Dr. Vander Willigen (Biochimie et Physiologie Moléculaire des Plantes, Montpellier, France) for critical reading of the manuscript.

Received May 3, 2005; revised July 13, 2005; accepted July 25, 2005; published September 23, 2005.

LITERATURE CITED

Aroca R, Amodeo G, Fernandez-Illescas S, Herman EM, Chaumont F, Chrispeels MJ (2005) The role of aquaporins and membrane damage in chilling and hydrogen peroxide induced changes in the hydraulic conductance of maize roots. Plant Physiol **137:** 341–353

Asamizu E, Nakamura Y, Sato S, Tabata S (2000) A large scale analysis of cDNA in *Arabidopsis thaliana*: generation of 12,028 non-redundant expressed sequence tags from normalized and size-selected cDNA libraries. DNA Res **7:** 175–180

Azaizeh H, Steudle E (1991) Effects of salinity on water transport of excised maize (*Zea mays* L.) roots. Plant Physiol **97:** 1136–1145

Barkla BJ, Vera-Estrella R, Pantoja O, Kirch HH, Bohnert HJ (1999) Aquaporin localization—how valid are the TIP and PIP labels? Trends Plant Sci **4:** 86–88

Bernard K, Auphan N, Granjeaud S, Victorero G, Schmitt-Verhulst AM, Jordan BR, Nguyen C (1996) Multiplex messenger assay: simultaneous, quantitative measurement of expression of many genes in the context of T cell activation. Nucleic Acids Res **24:** 1435–1442

Brown D (2003) The ins and outs of aquaporin-2 trafficking. Am J Physiol Renal Physiol **284:** F893–F901

Carpenter CD, Kreps JA, Simon AE (1994) Genes encoding glycine-rich *Arabidopsis thaliana* proteins with RNA-binding motifs are influenced by cold treatment and an endogenous circadian rhythm. Plant Physiol **104:** 1015–1025

Carvajal M, Martinez V, Alcaraz CF (1999) Physiological function of water channels as affected by salinity in roots of paprika pepper. Physiol Plant **105:** 95–101

Clough SJ, Bent AF (1998) Floral dip: a simplified method for *Agrobacterium*-mediated transformation of *Arabidopsis thaliana*. Plant J **16:** 735–743

Cutler SR, Ehrhardt DW, Griffitts JS, Somerville CR (2000) Random GFP:: cDNA fusions enable visualization of subcellular structures in cells of *Arabidopsis* at high frequency. Proc Natl Acad Sci USA **97:** 3718–3723

Desprez T, Amselem J, Caboche M, Höfte H (1998) Differential gene expression in *Arabidopsis* monitored using cDNA arrays. Plant J **14:** 643–652

Fetter K, Van Wilder V, Moshelion M, Chaumont F (2004) Interactions between plasma membrane aquaporins modulate their water channel activity. Plant Cell **16:** 215–228

Fricke W, Peters WS (2002) The biophysics of leaf growth in salt-stressed barley. A study at the cell level. Plant Physiol **129:** 374–388

Gerbeau P, Amodeo G, Henzler T, Santoni V, Ripoche P, Maurel C (2002) The water permeability of *Arabidopsis* plasma membrane is regulated by divalent cations and pH. Plant J **30:** 71–81

Gosti F, Bertauche N, Vartanian N, Giraudat J (1995) Abscisic acid-dependent and -independent regulation of gene expression by progressive drought in *Arabidopsis thaliana*. Mol Gen Genet **246:** 10–18

Guenther JF, Chanmanivone N, Galetovic MP, Wallace IS, Cobb JA, Roberts DM (2003) Phosphorylation of soybean nodulin 26 on serine 262 enhances water permeability and is regulated developmentally and by osmotic signals. Plant Cell **15:** 981–991

Halperin SJ, Gilroy S, Lynch JP (2003) Sodium chloride reduces growth and cytosolic calcium, but does not affect cytosolic pH, in root hairs of *Arabidopsis thaliana* L. J Exp Bot **54:** 1269–1280

Hasegawa PM, Bressan RA, Zhu J-K, Bohnert HJ (2000) Plant cellular and molecular responses to high salinity. Annu Rev Plant Physiol Plant Mol Biol **51:** 463–499

Higuchi T, Suga S, Tsuchiya T, Hisada H, Morishima S, Okada Y, Maeshima M (1998) Molecular cloning, water channel activity and tissue specific expression of two isoforms of radish vacuolar aquaporin. Plant Cell Physiol **39:** 905–913

Jang JY, Kim DG, Kim YO, Kim JS, Kang H (2004) An expression analysis of a gene family encoding plasma membrane aquaporins in response to abiotic stresses in Arabidopsis thaliana. Plant Mol Biol **54:** 713–725

Javot H, Lauvergeat V, Santoni V, Martin-Laurent F, Guclu J, Vinh J, Heyes J, Franck KI, Schaffner AR, Bouchez D, et al (2003) Role of a single aquaporin isoform in root water uptake. Plant Cell **15:** 509–522

Javot H, Maurel C (2002) The role of aquaporins in root water uptake. Ann Bot (Lond) **90:** 301–313

Johanson U, Karlsson M, Gustavsson S, Sjovall S, Fraysse L, Weig AR, Kjellbom P (2001) The complete set of genes encoding major intrinsic proteins in Arabidopsis provides a framework for a new nomenclature for major intrinsic proteins in plants. Plant Physiol **126:** 1358–1369

Johansson I, Karlsson M, Shukla VK, Chrispeels MJ, Larsson C, Kjellbom P (1998) Water transport activity of the plasma membrane aquaporin PM28A is regulated by phosphorylation. Plant Cell **10:** 451–460

Katsuhara M, Kuchitsu K, Takeshige K, Tazawa M (1989) Salt stress-induced cytoplasmic acidification and vacuolar alkalization in *Nitellopsis obtusa* cells. In vivo ^{31}P-nuclear magnetic resonance study. Plant Physiol **90:** 1102–1107

Kawasaki S, Borchert C, Deyholos M, Wang H, Brazille S, Kawai K, Galbraith D, Bohnert HJ (2001) Gene expression profiles during the initial phase of salt stress in rice. Plant Cell **13:** 889–905

Kirch H-H, Vera-Estrella R, Golldack D, Quigley F, Michalowski CB, Barkla BJ, Bohnert HJ (2000) Expression of water channel proteins in *Mesembryanthemum crystallinum*. Plant Physiol **123:** 111–124

Li L, Li S, Tao Y, Kitagawa Y (2000) Molecular cloning of a novel water channel from rice: its products expression in *Xenopus* oocytes and involvement in chilling tolerance. Plant Sci **154:** 43–51

Luu DT, Maurel C (2005) Aquaporins in a challenging environment: molecular gears for adjusting plant water status. Plant Cell Environ **28:** 85–96

Maathuis FJ, Filatov V, Herzyk P, Krijger GC, Axelsen KB, Chen S, Green BJ, Li Y, Madagan KL, Sanchez-Fernandez R, et al (2003) Transcriptome analysis of root transporters reveals participation of multiple gene families in the response to cation stress. Plant J **35:** 675–692

Martinez-Ballesta MC, Aparicio F, Pallas V, Martinez V, Carvajal M (2003) Influence of saline stress on root hydraulic conductance and PIP expression in *Arabidopsis*. J Plant Physiol **160:** 689–697

Martinez-Ballesta MC, Martinez V, Carvajal M (2000) Regulation of water channel activity in whole roots and in protoplasts from roots of melon plants grown under saline conditions. Aust J Plant Physiol **27:** 685–691

Martre P, Morillon R, Barrieu F, North GB, Nobel PS, Chrispeels MJ (2002) Plasma membrane aquaporins play a significant role during recovery from water deficit. Plant Physiol **130:** 2101–2110

Maurel C, Javot H, Lauvergeat V, Gerbeau P, Tournaire C, Santoni V, Heyes J (2002) Molecular physiology of aquaporins in plants. Int Rev Cytol **215:** 105–148

Maurel C, Kado RT, Guern J, Chrispeels MJ (1995) Phosphorylation regulates the water channel activity of the seed-specific aquaporin α-TIP. EMBO J **14:** 3028–3035

Munns R, Passioura JB (1984) Hydraulic resistance of plants. III. Effects of NaCl in barley and lupin. Aust J Plant Physiol **11:** 351–359

Murashige T, Skoog F (1962) A revised medium for rapid growth and bioassays with tobacco tissue cultures. Physiol Plant **15:** 473–497

Passioura JB (1988) Water transport in and to roots. Annu Rev Plant Physiol Plant Mol Biol **39:** 245–265

Pérez-Amador MA, Lidder P, Johnson MA, Landgraf J, Wisman E, Green PJ (2001) New molecular phenotypes in the *dst* mutants of Arabidopsis revealed by DNA microarray analysis. Plant Cell **13:** 2703–2717

Peyrano G, Taleisnik E, Quiroga M, de Forchetti SM, Tigier H (1997) Salinity effects on hydraulic conductance, lignin content and peroxydase activity in tomato roots. Plant Physiol Biochem **35:** 387–393

Quigley F, Rosenberg JM, Shachar-Hill Y, Bohnert HJ (2001) From genome to function: the *Arabidopsis* aquaporins. Genome Biol **3:** 1–17

Saito C, Ueda T, Abe H, Wada Y, Kuroiwa T, Hisada A, Furuya M, Nakano A (2002) A complex and mobile structure forms a distinct subregion within the continuous vacuolar membrane in young cotyledons of *Arabidopsis*. Plant J **29:** 245–255

Santoni V, Vinh J, Pflieger D, Sommerer N, Maurel C (2003) A proteomic study reveals novel insights into the diversity of aquaporin forms

expressed in the plasma membrane of plant roots. Biochem J **372:** 289–296

Siefritz F, Tyree MT, Lovisolo C, Schubert A, Kaldenhoff R (2002) PIP1 plasma membrane aquaporins in tobacco: from cellular effects to function in plants. Plant Cell **14:** 869–876

Smart LB, Moskal WA, Cameron KD, Bennett AB (2001) MIP genes are down-regulated under drought stress in *Nicotiana glauca.* Plant Cell Physiol **42:** 686–693

Steudle E (2000) Water uptake by roots: effects of water deficit. J Exp Bot **51:** 1531–1542

Suga S, Imagawa S, Maeshima M (2001) Specificity of the accumulation of mRNAs and proteins of the plasma membrane and tonoplast aquaporins in radish organs. Planta **212:** 294–304

Suga S, Komatsu S, Maeshima M (2002) Aquaporin isoforms responsive to salt and water stresses and phytohormones in radish seedlings. Plant Cell Physiol **43:** 1229–1237

Thomine S, Lelievre F, Debarbieux E, Schroeder JI, Barbier-Brygoo H (2003) AtNRAMP3, a multispecific vacuolar metal transporter involved in plant responses to iron deficiency. Plant J **34:** 685–695

Tournaire-Roux C, Sutka M, Javot H, Gout E, Gerbeau P, Luu DT, Bligny R, Maurel C (2003) Cytosolic pH regulates root water transport during anoxic stress through gating of aquaporins. Nature **425:** 393–397

Tyerman SD, Oats P, Gibbs J, Dracup M, Greenway H (1989) Turgor-volume regulation and cellular water relations of *Nicotiana tabacum* roots grown in high salinities. Austr J Plant Physiol **16:** 517–531

Vera-Estrella R, Barkla BJ, Bohnert HJ, Pantoja O (2004) Novel regulation of aquaporins during osmotic stress. Plant Physiol **135:** 2318–2329

Weig A, Deswarte C, Chrispeels MJ (1997) The major intrinsic protein family of Arabidopsis has 23 members that form three distinct groups with functional aquaporins in each group. Plant Physiol **114:** 1347–1357

Xu W, Bak S, Decker A, Paquette SM, Feyereisen R, Galbraith DW (2001) Microarray-based analysis of gene expression in very large gene families: the cytochrome P450 gene superfamily of *Arabidopsis thaliana.* Gene **272:** 61–74

Yamada S, Katsuhara M, Kelly WB, Michalowski CB, Bohnert HJ (1995) A family of transcripts encoding water channel proteins: tissue-specific expression in the common ice plant. Plant Cell **7:** 1129–1142

Yamaguchi-Shinozaki K, Shinozaki K (1993) Characterization of the expression of a desiccation-responsive *rd29* gene of *Arabidopsis thaliana* and analysis of its promoter in transgenic plants. Mol Gen Genet **236:** 331–340

Zhu J-K (2003) Regulation of ion homeostasis under salt stress. Curr Opin Plant Biol **6:** 441–445

Zhu J-K, Liu J, Xiong L (1998) Genetic analysis of salt tolerance in Arabidopsis: evidence for a critical role of potassium nutrition. Plant Cell **10:** 1181–1191